Hybrid Active Noise Control Structures: A Short Overview

Piero Rivera Benois, Patrick Nowak, and Udo Zölzer

Dept. of Signal Processing and Communications, Helmut Schmidt University, Hamburg, Germany
Email: {piero.rivera.benois,patrick.nowak,udo.zoelzer}@hsu-hh.de

Abstract

The classical feedforward and feedback active noise control structures can be combined in pairs into hybrid control systems, in order to partially compensate for their individual limitations. The increase in complexity is compensated by the flexibility and attenuation performance they can achieve together. Several combination strategies can be found in the literature in different application contexts and formulated using different nomenclatures. This paper provides a single source for the existing hybrid control structures in a purely digital implementation. For each one of them a block diagram in context of active noise control headphones is provided. To describe the interaction between the classical structures within the hybrid system, changes in the transfer functions and effective plants are discussed.

1 Introduction

Active noise control (ANC) technology aims to reduce the sound pollution present in the environment by actively generating sound pressure waves that overlap destructively on a sweet-spot with the ones of the noise sources. In order to achieve a perfect attenuation, the phase and the magnitude of the noise around the sweet-spot have to be matched. Different approaches can be used to achieve this, depending on the nature of the noise and the solution's context.

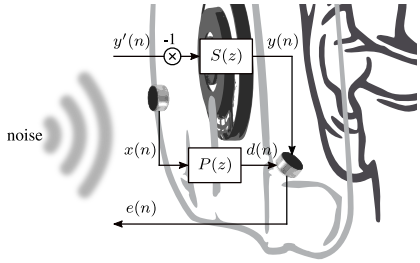

Figure 1: Signals and systems around ANC headphones

In the general case of ANC headphones, the transducers and systems presented in Fig. 1 can be found. An external microphone measures a time-advanced reference of the incoming disturbance $x(n)$. This signal is measured again as $d(n)$, after it has entered the ear-cup and reached the so-called error microphone. Thus, $P(z)$, known as the primary path, is defined as the changes in magnitude and phase that the disturbance suffers by means of the headphone's construction materials and its angle of incidence. The control signal $y'(n)$ generated by the ANC system is digitally sign-inverted, fed to the speaker and measured again by the error microphone as $y(n)$. Hence, the loudspeaker and the error microphone define the so-called secondary path $S(z)$, which considers the characteristics of both elements plus the acoustic path between them. At the end, the control signal $y(n)$ and the disturbance $d(n)$ overlap destructively at the error microphone's position, and the residual error $e(n)$ is generated.

ANC approaches that use the residual error $e(n)$ for calculating $y'(n)$ are called feedback control schemes. On the other hand, the ones that use the time-advanced reference signal $x(n)$ for calculating $y'(n)$ are called feedforward or forward control schemes. Adaptive implementations of feedforward controllers also utilize $e(n)$ to solve the underlying optimization problem.

In the following section, three classical control structures are introduced in a digital implementation context. Afterwards, the hybrid structures are described, which combine two of the classical control structures into one system. At the end, conclusions are drawn based on the interdependencies and changes observed in the six different hybrid control structures.

2 Classical Control Structures

The Minimum Variance Control utilizes the less expensive control structure [1]. Its block diagram is presented in Fig. 2. Here, the controller $W_\mathrm{m}(z)$ is designed to minimize the variance of the residual error $e(n)$, by means of a negative acoustic feedback built through $S(z)$.

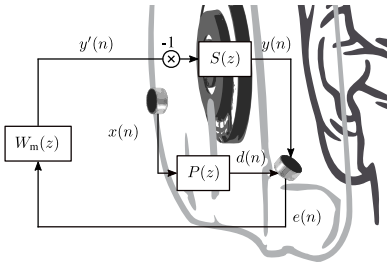

Figure 2: The Minimum Variance Control structure.

The feedback generates a transfer function

$$H_\mathrm{m}(z) = \frac{E(z)}{D(z)} = \frac{1}{1 + S(z) \cdot W_\mathrm{m}(z)}, \tag{1}$$

which magnitude decreases under the proper design of the product $S(z) \cdot W_\mathrm{m}(z)$. The design of it comprises an optimization problem under stability and performance constraints, which are well documented in [2] and [3]. The reachable attenuation bandwidth of this structure is limited by the delays within the control loop. Because of this, most of its early implementations were done using analog circuits, so to avoid the AD and DA conversion delays.

In order to partially overcome the attenuation bandwidth limitation of the MVC, and extend the attenuation capabilities of the feedback system to tonal components, a digital feedback control scheme called Internal Model Control (IMC) can be used [1]. Its block diagram is presented in Fig. 3. The control scheme uses an estimation of

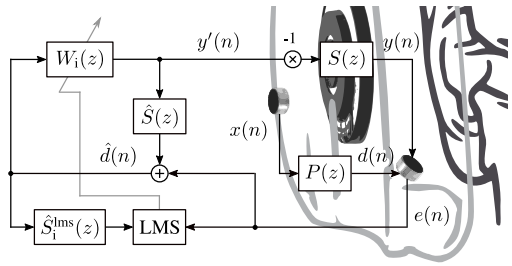

Figure 3: The Internal Model Control structure based on the FxLMS adaptation algorithm.

the secondary path $\hat{S}(z)$ to estimate $d(n)$, by compensating the influence of the control signal $y'(n)$ in the residual error $e(n)$.

The system's transfer function

$$H_{\mathrm{i}}(z) = \frac{E(z)}{D(z)} = \frac{1 - \hat{S}(z) \cdot W_{\mathrm{i}}(z)}{1 + \big(S(z) - \hat{S}(z)\big) \cdot W_{\mathrm{i}}(z)} \tag{2}$$

shows a denominator similar to the one of (1), which reduces to 1 if $\hat{S}(z) = S(z)$ holds. Under this consideration the system behaves like a feedforward one. Because this condition can not always be ensured, stability and performance constraints still have to be considered when designing $W_{\mathrm{i}}(z)$ [3]. An implementation based on an FxLMS algorithm, like the one presented in Fig. 3, requires an estimation of the effective secondary path $\hat{S}_{\mathrm{i}}^{\mathrm{lms}}(z) = -\frac{E(z)}{Y'(z)}$ seen from the controller's perspective.

In contexts where a time-advanced reference can be provided, a feedforward control scheme (FF) can be used [4]. As illustrated in Fig. 4, the reference signal $x(n)$ outside of the ear-cup is used by the controller $W_{\mathrm{f}}(z)$ to generate $y'(n)$. This control signal is sign-inverted and then fed to the secondary path, so it destructively overlaps with $d(n)$ at the error microphone's position. The residual error $e(n)$ is then used for solving the optimization of the filter coefficients of $W_{\mathrm{f}}(z)$, which is in most cases implemented as an FIR filter.

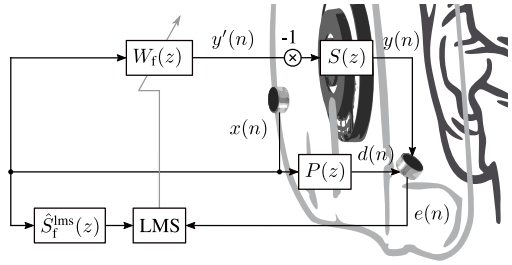

Figure 4: The feedforward control structure based on the FxLMS adaptation algorithm.

The system's transfer function

$$H_{\mathrm{f}}(z) = \frac{E(z)}{X(z)} = P(z) - S(z) \cdot W_{\mathrm{f}}(z) \tag{3}$$

considers the passive and active attenuations suffered by the disturbance $x(n)$ until it reaches the error microphone's position. It also defines the underlying causality problem, i.e. the digital delay of the controller $W_{\mathrm{f}}(z)$ plus the acoustical delay of $S(z)$ has to be smaller or equal to the acoustic delay of $P(z)$. If this constraint is met, then the optimal solution for $W_{\mathrm{f}}(z)$

$$W_{\mathrm{f}}^{\mathrm{opt}}(z) = \frac{P(z)}{S(z)} \tag{4}$$

can be used. Because the control signal calculation relies on the information contained in the reference signal, only disturbances correlated with it can be attenuated. Therefore, the maximum achievable attenuation is limited by the cross-correlation between $x(n)$ and $d(n)$ [4].

3 Hybrid Control Structures

The control structures presented in this section aim to combine the attenuation capabilities of two classical digital structures into a single system. Every combination has two alternatives, i.e. one that produces independent optimal solutions for its controllers and another one, which creates a dependency between them. Their system transfer functions and the changes they introduce in the effective primary and secondary paths are utilized to understand these behaviors.

3.1 Minimum Variance Control combined with Internal Model Control

The MVC-IMC combination proposed in [5] for a digital IMC and analog MVC implementation, got simplified later on in [6] by a fully digital implementation of it. The resulting system diagram is presented in Fig. 5a. In the bottom part the IMC structure can be seen. The estimated signal $\hat{e}_{\mathrm{m}}(n)$ is an estimation of the residual error left by the MVC. The IMC and the MVC controllers (W_{i}(z) and W_{m}(z), respectively) are connected in parallel for generating individual control signals, which are summed up and sing-inverted before they are fed to the secondary path. The system's transfer function

$$H_{\mathrm{mi}}(z) = \frac{E(z)}{D(z)} = \frac{1 - \hat{S}(z) W_{\mathrm{i}}(z)}{1 + S(z) W_{\mathrm{m}}(z) + \big(S(z) - \hat{S}(z)\big) W_{\mathrm{i}}(z)} \tag{5}$$

presents the numerator of (2) and a denominator that is almost an additive combination of the ones of (1) and (2). If $\hat{S}(z) = S(z)$ holds, then the denominator reduces to the one in (1), and both controllers can be designed independently. However, no stability and performance analysis can be found in the literature regarding what happens if this condition is not met. Thus, a more reliable design method for these controllers still has to be developed. The effective secondary path seen by the IMC controller

$$\hat{S}_{\mathrm{i}}^{\mathrm{lms}}(z) = -\frac{E(z)}{Y_{\mathrm{i}}'(z)} = S(z) \frac{1 + \hat{S}(z) W_{\mathrm{m}}(z)}{1 + S(z) W_{\mathrm{m}}(z)} \tag{6}$$

can be calculated by considering $d(n) = 0$, $y_{\mathrm{i}}'(n)$ as the input to the system, and $e(n)$ as its output. As it can be seen, the effective secondary path shows an asymptotic behavior between $S(z)$ and $\hat{S}(z)$ regarding the magnitude of $W_{\mathrm{m}}(z)$. Thus, it approximates $\hat{S}(z)$ in frequencies where $|W_{\mathrm{m}}(z)| \gg 1$, and on the other hand $S(z)$, when $|W_{\mathrm{m}}(z)| \ll 1$. By doing so, the magnitude of $W_{\mathrm{m}}(z)$ may partially help the adaptation algorithm to overcome mismatches between $S(z)$ and $\hat{S}(z)$.

3.1.1 Alternative structure with dependent internal model control optimum

An alternative IMC-MVC combination can be found earlier in the literature [7–10]. The block diagram of it is presented in Fig. 5b. Here the MVC uses directly the error

signal $e(n)$ for calculating $y'_{\mathrm{m}}(n)$, which alters the effective secondary path seen from the IMC perspective

$$\hat{S}_{\mathrm{i}}^{\mathrm{lms}}(z) = -\frac{E(z)}{Y'_{\mathrm{i}}(z)} = \frac{S(z)}{1+S(z)W_{\mathrm{m}}(z)}. \tag{7}$$

This change is considered beneficial for the IMC, because under certain conditions $\frac{S(z)}{1+S(z)W_{\mathrm{m}}(z)}$ is easier to control and model than $S(z)$ [8]. Furthermore, if $\hat{S}_{\mathrm{i}}(z) = \frac{\hat{S}(z)}{1+\hat{S}(z)W_{\mathrm{m}}(z)}$ is chosen, then the system's transfer function (omitting the argument z) yields

$$H_{\mathrm{mido}} = \frac{1+\hat{S}\cdot W_{\mathrm{m}} - \hat{S}\cdot W_{\mathrm{i}}}{1+(S+\hat{S})\cdot W_{\mathrm{m}} + S\cdot\hat{S}\cdot W_{\mathrm{m}}^2 + (S-\hat{S})\cdot W_{\mathrm{i}}}. \tag{8}$$

The denominator can be interpreted as the approximation of a squared binomial with a residual. The residual can be zero, under which circumstances $\hat{S}(z) = S(z)$ would hold and the system's transfer function would simplify to

$$H_{\mathrm{mido}}(z) = \frac{1-\frac{S(z)}{1+S(z)W_{\mathrm{m}}(z)}W_{\mathrm{i}}(z)}{1+S(z)W_{\mathrm{m}}(z)}. \tag{9}$$

As it can be seen by comparing with (5), the change in the effective secondary path alters mainly the influence of $W_{\mathrm{i}}(z)$. This influence of the MVC over the control effort of the IMC is what is understood as the dependent internal model control optimum. However, a stability and performance analysis has to be carried out, in order to design controllers for this specific structure, as in many applications $\hat{S}(z)$ deviates significantly from $S(z)$.

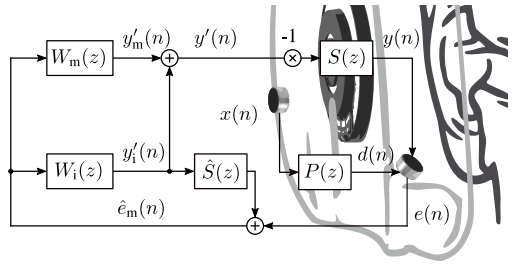

(a) MVC-IMC combination with independent optima

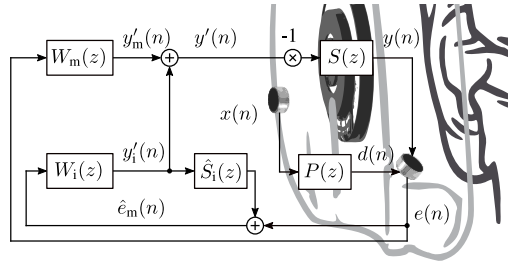

(b) MVC-IMC combination with dependent optima

Figure 5: Hybrid control structures involving the combination of the MVC with the IMC approaches: (a) the structure with independent IMC optimal controller, and (b) the structure with dependent IMC optimal controller.

3.2 Minimum Variance Control combined with Feedforward Control

In solutions where the electronics of an adaptive feedforward control are available, an MVC controller can improve the attenuation performance, without significantly incrementing the implementation effort. The block diagram presented in Fig. 6a depicts the MVC-FF combination suggested in [11–14]. The MVC and FF controllers ($W_{\mathrm{m}}(z)$ and $W_{\mathrm{f}}(z)$, respectively) work independent from each others. The reference signal $x(n)$ and error signal $e(n)$ are used to calculate the control signals $y'_{\mathrm{f}}(n)$ and $y'_{\mathrm{m}}(n)$ in parallel. The addition of both signals $y'(n)$ is sign-inverted and then fed to the secondary path. The system's transfer function

$$H_{\mathrm{fm}}(z) = \frac{E(z)}{X(z)} = \frac{P(z)-S(z)W_{\mathrm{f}}(z)}{1+S(z)W_{\mathrm{m}}(z)} \tag{10}$$

reflects a combined passive and active attenuation effect, where the controllers work independent from each other. Thus, a multiplicative combination of (3) and (1) can be seen. Due to the MVC control loop, the effective secondary path

$$\hat{S}_{\mathrm{f}}^{\mathrm{lms}}(z) = -\frac{E(z)}{Y'_{\mathrm{f}}(z)} = \frac{S(z)}{1+S(z)W_{\mathrm{m}}(z)} \tag{11}$$

seen between the feedforward control signal $y'_{\mathrm{f}}(n)$ and the error signal $e(n)$ changes to the same expression found in (7). Thus, this structure may profit from an effective secondary path that is easier to control and model.

3.2.1 Alternative structure with dependent feedforward optimum

An alternative to the previous structure is found in the literature later on in [15, 16]. In Fig. 6b the block diagram of the structure is presented. An approximation of the secondary path $\hat{S}(z)$ is used to make an estimation of $y'_{\mathrm{f}}(n)$ at the error microphone's position $\hat{y}_{\mathrm{f}}(n)$. This estimation is used to negate the effect of the FF in the error signal $e(n)$, before this is used by the MVC for calculating $y'_{\mathrm{m}}(n)$. By doing so, the effective secondary path seen from the FF perspective

$$\hat{S}_{\mathrm{f}}^{\mathrm{lms}}(z) = -\frac{E(z)}{Y'_{\mathrm{f}}(z)} = S(z)\frac{1+\hat{S}(z)W_{\mathrm{m}}(z)}{1+S(z)W_{\mathrm{m}}(z)} \tag{12}$$

changes to the one already seen in (6), and produces a change in the system's transfer function

$$H_{\mathrm{fmdo}}(z) = \frac{P(z)}{1+S(z)W_{\mathrm{m}}(z)} - S(z)W_{\mathrm{f}}(z)\frac{1+\hat{S}(z)W_{\mathrm{m}}(z)}{1+S(z)W_{\mathrm{m}}(z)}. \tag{13}$$

The change can be interpreted as a change in the effective primary path $P(z)$ by the transfer function of the MVC. Furthermore, if the optimal solution of $W_{\mathrm{f}}(z)$

$$W_{\mathrm{f}}^{\mathrm{opt}}(z) = \frac{P(z)}{S(z)}\cdot\frac{1}{1+\hat{S}(z)W_{\mathrm{m}}(z)}, \tag{14}$$

is derived from $H_{\mathrm{fmdo}}(z)$, then a decrease in the FF control effort can be found in regions where the MVC is effective. Thus, the new FF optimum may target a frequency region where the MVC attenuation is not dominant. This effect is the cause for the dependent feedforward optimum.

3.3 Internal Model Control combined with Feedforward Control

The IMC-FF combination [17–20] offers the possibility to design both feedforward and feedback controllers based on Wiener filter formulations or on similar adaptation algorithms. In Fig. 7a an illustration of its block diagram is

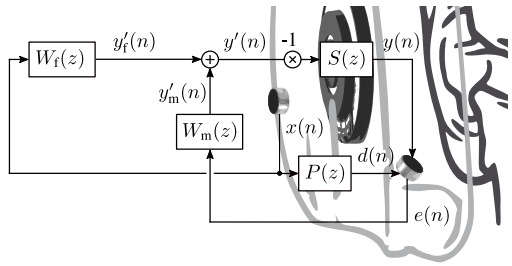

(a) MVC-FF combination with independent optima

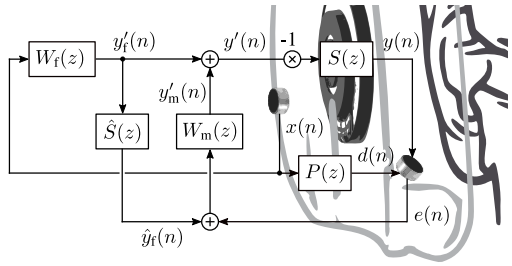

(b) MVC-FF combination with dependent optima

Figure 6: Hybrid control structures involving the combination of the MVC with the FF approaches: (a) the structure with independent FF optimal controller, and (b) the structure with dependent FF optimal controller.

presented. On top, the FF controller $W_\mathrm{f}(z)$ is fed with the reference signal $x(n)$, and its output $y'_\mathrm{f}(n)$ is added to the control signal $y'_\mathrm{i}(n)$ generated by the IMC controller $W_\mathrm{i}(z)$. The result of the sum $y'(n)$ is fed to the secondary path $S(z)$. In parallel, $y'_\mathrm{i}(n)$ is convolved with a model of the secondary path $\hat{S}(z)$. The result of the convolution is used afterwards to negate the influence of the IMC in the error signal $e(n)$. By doing so, an estimate of the error left by the FF $\hat{e}_\mathrm{f}(n)$ is calculated. This estimate is used as input for $W_\mathrm{i}(z)$. Then the system's transfer function

$$H_\mathrm{fi}(z) = \frac{E(z)}{X(z)} = \frac{\big(P(z) - S(z)W_\mathrm{f}(z)\big)\cdot\big(1-\hat{S}(z)W_\mathrm{i}(z)\big)}{1+\big(S(z)-\hat{S}(z)\big)W_\mathrm{i}(z)} \tag{15}$$

yields the multiplicative combination of (3) and (2). So $W_\mathrm{f}(z)$ and $W_\mathrm{i}(z)$ can be designed independently. Nevertheless, for an adaptive implementation of $W_\mathrm{f}(z)$, the effective secondary path seen from its perspective

$$\hat{S}_\mathrm{f}^\mathrm{lms}(z) = -\frac{E(z)}{Y'_\mathrm{f}(z)} = S(z)\frac{1-\hat{S}(z)W_\mathrm{i}(z)}{1+\big(S(z)-\hat{S}(z)\big)W_\mathrm{i}(z)} \tag{16}$$

has to be considered. As it can be seen, now the effective secondary path has to be continuously monitored upon changes of $W_\mathrm{i}(z)$ and mismatches between $S(z)$ and $\hat{S}(z)$.

3.3.1 Alternative structure with dependent feedforward optimum

An alternative to the previous IMC-FF combination [4, 21–24] partially circumvents the monitoring of $\hat{S}_\mathrm{f}^\mathrm{lms}(z)$, based on a small change. The block diagram in Fig. 7b illustrates it. By adding first $y'_\mathrm{f}(n)$ and $y'_\mathrm{i}(n)$ and using its result $y'(n)$ later for the convolution with $\hat{S}(z)$ in the IMC, the effective secondary path of FF changes to

$$\hat{S}_\mathrm{f}^\mathrm{lms}(z) = -\frac{E(z)}{Y'_\mathrm{f}(z)} = \frac{S(z)}{1+\big(S(z)-\hat{S}(z)\big)W_\mathrm{i}(z)}. \tag{17}$$

As a direct effect of this change, the effective secondary path is almost independent of $W_\mathrm{i}(z)$ and only the mismatch between $S(z)$ and $\hat{S}(z)$ has to be monitored. The change also alters the system's transfer function

$$H_\mathrm{fido}(z) = \frac{P(z)\cdot\big(1-\hat{S}(z)W_\mathrm{i}(z)\big) - S(z)W_\mathrm{f}(z)}{1+\big(S(z)-\hat{S}(z)\big)W_\mathrm{i}(z)}, \tag{18}$$

which now shows a dependency between the $W_\mathrm{f}(z)$ and $W_\mathrm{i}(z)$. If $H_\mathrm{fido}(z) = 0$ is set, the optimal solution for $W_\mathrm{f}(z)$

$$W_\mathrm{f}^\mathrm{opt}(z) = \frac{P(z)}{S(z)}\cdot\big(1-\hat{S}(z)W_\mathrm{i}(z)\big) \tag{19}$$

can be derived. By comparing (19) with (4), one can see that the control performance achieved by the feedback controller $W_\mathrm{i}(z)$ changes the effective primary path, and with it the control effort of $W_\mathrm{f}(z)$. This influence may steer the FF optimum in the same way it was seen in Subsection 3.2.1.

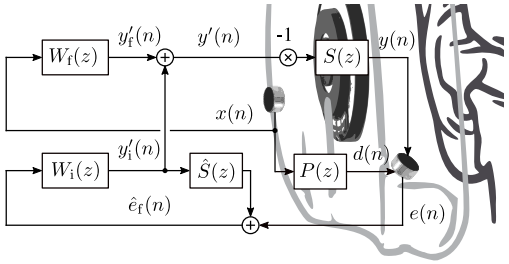

(a) IMC-FF combination with independent optima

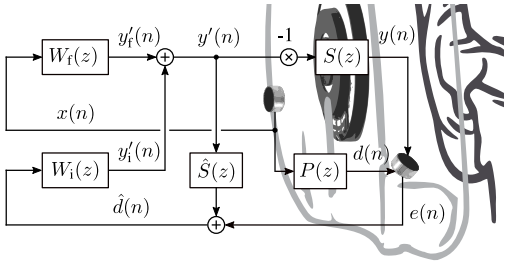

(b) IMC-FF combination with dependent optima

Figure 7: Hybrid control structures involving the combination of the IMC with the FF approaches: (a) the structure with independent FF optimal controller, and (b) the structure with dependent FF optimal controller.

4 Conclusions

In this work an overview of the six possible combinations of the classical control structures for active noise control is presented. With MVC-IMC combinations one can have a system which performance is more robust to moving noise sources. Nevertheless, the stability analysis regarding deviations of the estimated secondary path from the real one is still to be developed. With IMC-FF combinations one could profit from two adaptive controllers working together. However, this requires a continuous monitoring of the effective secondary path, so that the adaptation of the FF controller remains stable. Finally, with MVC-FF combinations the stability and performance considerations relies on the analysis of the MVC only. Moreover, the MVC-FF combination with dependent FF optimum may steer the FF to find an optimal solution in frequency regions where this feedback approach is not effective anymore.

References

[1] S. J. Elliott, "Design and performance of feedback controllers," in *Signal Processing for Active Control* (S. J. Elliott, ed.), Signal Processing and its Applications, ch. 6, London: Academic Press, 2001.

[2] M. Pawełczyk, "Analogue active noise control," *Applied Acoustics*, vol. 63, no. 11, pp. 1193 – 1213, 2002.

[3] B. Rafaely, *Feedback Control of Sound*. PhD thesis, University of Southampton, Southampton, England, 1997.

[4] K. M. Sen and D. R. Morgan, *Active Noise Control Systems: Algorithms and DSP Implementations*. Telecommunications and Signal Processing, New York: John Wiley & Sons, Inc, 1996.

[5] T. Schumacher, H. Krüger, M. Jeub, P. Vary, and C. Beaugeant, "Active noise control in headsets: A new approach for broadband feedback ANC," in *2011 IEEE International Conference on Acoustics, Speech and Signal Processing (ICASSP)*, pp. 417–420, May 2011.

[6] P. Rivera Benois, P. Nowak, and U. Zölzer, "Fully Digital Implementation of a Hybrid Feedback Structure for Broadband Active Noise Control in Headphones," in *2017 Proceedings of the 24th International Congress on Sound and Vibration*, July 2017.

[7] T. Tay and J. Moore, "Enhancement of fixed controllers via adaptive-q disturbance estimate feedback," *Automatica*, vol. 27, no. 1, pp. 39 – 53, 1991.

[8] S. J. Elliott, "Adaptive feedback controllers," in *Signal Processing for Active Control* (S. J. Elliott, ed.), Signal Processing and its Applications, ch. 7, London: Academic Press, 2001.

[9] M. Pawełczyk, "A hybrid active noise control system," *Archives of Control Sciences*, vol. 13, no. 2, pp. 191–213, 2003.

[10] Y. Song, Y. Gong, and S. M. Kuo, "A robust hybrid feedback active noise cancellation headset," *IEEE Transactions on Speech and Audio Processing*, vol. 13, pp. 607–617, July 2005.

[11] C. Carme, "The third principle of active control: The feed forback," *INTER-NOISE and NOISE-CON Congress and Conference Proceedings*, vol. 1999, no. 5, pp. 885–896, 1999.

[12] B. Rafaely and M. Jones, "Combined feedback-feedforward active noise-reducing headset–the effect of the acoustics on broadband performance," *The Journal of the Acoustical Society of America*, vol. 112, no. 3, pp. 981–989, 2002.

[13] L. Håkansson, S. Johansson, M. Dahl, P. Sjisten, and I. Claesson, "Noise cancelling headsets for speech communication," in *Noise Reduction in Speech Applications* (G. M. Davis, ed.), ch. 12, pp. 305–328, London: CRC Press, 2002.

[14] A. D. Streeter, L. R. Ray, and R. D. Collier, "Hybrid feedforward-feedback active noise control," in *Proceedings of the 2004 American Control Conference*, vol. 3, pp. 2876–2881 vol.3, June 2004.

[15] H. Foudhaili, *Kombinierte feedback- und adaptive Feedforward-Regelung für aktive Lärmreduktion in einem Kommunikations-Headset*. PhD thesis, Leibniz Universitä Hannover, Aachen, 2008.

[16] P. Rivera Benois, V. Papantoni, and U. Zölzer, "Psychoacoustic Hybrid Active Noise Control Structure for Application in Headphones," in *2018 Proceedings of the 25th International Congress on Sound and Vibration*, July 2018.

[17] X. Kong, P. Liu, and S. M. Kuo, "Multiple channel hybrid active noise control systems," *IEEE Transactions on Control Systems Technology*, vol. 6, pp. 719–729, Nov 1998.

[18] C. H. Hansen, *Understanding Active Noise Cancellation*. London: Spon Press, 2001.

[19] L. Wu, X. Qiu, I. S. Burnett, and Y. Guo, "Decoupling feedforward and feedback structures in hybrid active noise control systems for uncorrelated narrowband disturbances," *Journal of Sound and Vibration*, vol. 350, pp. 1 – 10, 2015.

[20] P. Rivera Benois, P. Nowak, and U. Zölzer, "Evaluation of a decoupled feedforward-feedback hybrid structure for active noise control headphones in a multi-source environment," in *Proceedings of the 46th International Congress and Exposition on Noise Control Engineering, INTER-NOISE*, Aug 2017.

[21] S. Johansson, M. Winberg, T. Lagö, and I. Claesson, "A New Active Headset For a Helicopter Application," in *1997 Proceedings of the 5th International Congress on Sound and Vibration*, December 1997.

[22] W.-K. Tseng, B. Rafaely, and S. J. Elliott, "Combined feedback-feedforward active control of sound in a room," *The Journal of the Acoustical Society of America*, vol. 104, no. 6, pp. 3417–3425, 1998.

[23] Y.-K. Chong, L. Wang, S.-C. Ting, and W.-S. Gan, "Integrated headsets using the adaptive hybrid active noise control system," in *2005 5th International Conference on Information Communications Signal Processing*, pp. 1324–1328, 2005.

[24] T. Wang, W. S. Gan, and Y. K. Chong, "Psychoacoustic hybrid active noise control system," in *2012 IEEE International Conference on Acoustics, Speech and Signal Processing (ICASSP)*, pp. 321–324, March 2012.